

ANALYSIS OF ARTIFACTS IN SUB-PIXEL REMOTE SENSING IMAGE REGISTRATION

Jordi Inglada¹, Vincent Muron², Damien Pichard² and Thomas Feuvrier²

¹CNES - DCT/SI/AP

18, Av. E. Belin, 31401 Toulouse Cedex 9, France.

²CS-SI, Space Division

Rue Brindejonc des Moulinais, BP 5872, 31506 Toulouse Cedex 5, France.

KEY WORDS: Interpolation artifacts, image registration, disparity map, similarity measure.

ABSTRACT:

Sub-pixel accuracy image registration is needed for many applications. In order to achieve this accuracy, one uses image re-sampling. Since the image interpolation step is performed a high number of times, approximate interpolations are performed in order to reduce computation cost. In this paper we study the artifacts introduced in the disparity map estimation by the approximate interpolation and propose strategies in order to reduce them.

1. INTRODUCTION

SUB-PIXEL accuracy image registration is needed for applications such as change detection, Pan-Sharpening, and data fusion. In order to achieve this accuracy, the deformation between the two images to be registered is usually modeled by a displacement vector field which can be estimated by measuring rigid local shifts for each pixel in the image.

In order to measure subpixel shifts, image resampling is used. Sampling theory says that, if a continuous signal has been sampled according to the Nyquist criterion, a perfect continuous reconstruction can be obtained from the sampled version. Therefore, a shifted version of a sampled signal can be obtained by interpolation and resampling with a shifted origin.

Since only a sampled version of the shifted signal is needed, the reconstruction needs only to be performed for the new positions of the samples, so the whole procedure comes to computing the value of the signal for the new sample positions.

In the case of image registration, the similarity between the reference image and the shifted versions of the image to be registered is measured assuming that the maximum of similarity determines the most likely shift. The image interpolation step is thus performed a high number of times during the similarity optimization procedure. In order to reduce computation cost, approximate interpolations are performed. Indeed, the ideal interpolator is a sinus cardinal function, and therefore, an infinite number of samples is needed for the computation of any new sample. Several approaches exist for reducing the computation time. For instance, a truncated Sinc interpolator needs only a few samples. Other interpolators like the linear one can also be used.

Approximate interpolators will introduce errors in the resampled image which may induce errors in the similarity measure and therefore produce errors in the estimated shifts.

This paper addresses the following points:

1. The characterization of the artifacts for different similarity measures and interpolators.
2. The theoretical explanation of the origin of the artifacts.
3. Some guidelines and recommendations in order to attenuate these artifacts.

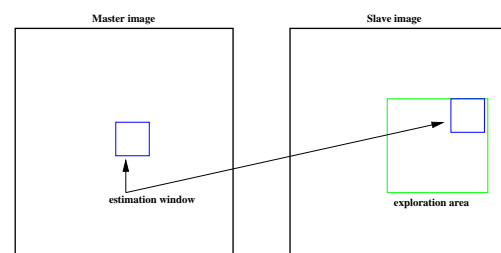


Figure 1. Estimation of the similarity surface.

2. DISPARITY MAP ESTIMATION

In this section, we recall the principle of disparity map estimation used in order to achieve subpixel accuracy.

The geometric deformation is modeled by local rigid displacements (Inglada and Giros, 2004). One wants to estimate the coordinates of each pixel of the reference image inside the secondary image. This can be represented by a displacement vector associated to every pixel of the reference image. Each of the two components (lines and columns) of this vector field will be called deformation grid.

We use a small window taken in the reference image and we test the similarity for every possible shift within an exploration area inside the secondary image (fig. 1). That means that for each position we compute the similarity measure. The result is a similarity surface whose maximum gives the most likely local shift between both images.

Quality criteria can be applied to the estimated maximum in order to give a confidence factor to the estimated shift: width of the peak, maximum value, etc. Sub-pixel shifts can be measured by applying fractional shifts to the sliding window. This is done by image interpolation. The interesting parameters of the procedure are:

- The size of the exploration area: it determines the computational load of the algorithm (we want to reduce it), but it has to be large enough in order to cope with large deformations.
- The size of the sliding window: the robustness of the similarity measure estimation increases with the window size, but the hypothesis of local rigid shifts may not be valid for large windows.

3. ASSESSMENT OF THE ARTIFACTS

In this section, we introduce the problem of subpixel shift artifacts by analysing the results obtained in a real case. Our data set consists in the following pair (a region of a size of 2000×2000 pixels is used for our tests):

- the B3 channel of a Spot 4 image (20 m pixel resolution) acquired on June 24, 2001 over the East of the Bucharest area (figure 2(a));
- a ERS-2 SAR 3-looks intensity image (12.5 m pixel size and approximately 20 m pixel resolution) acquired on May 10, 2001 over the same area (figure 2(b)).

Both images were ortho-rectified: for the Spot 4 image a digital elevation model (DEM) (figure 2(c)) with an altimetric precision better than 10 m and a planimetric precision around 10 m has been used, together with the acquisition model (orbits, attitude) for the satellite; for the ERS-2 image no DEM was used, but a constant altitude and homologous points manually taken on the Spot 4 image were used in the ortho-rectification process. Globally, the images show a good superposition, but local errors exist, which can amount several pixels due to the simple geometric modeling of the deformation of the radar image. If we analyze the DEM, we see that a gentle slope descending from NW to SE exists and that abrupt topography features appear in the NE and the SW. The shape of the river can also be identified in the DEM.

Fig. 3 presents the horizontal and vertical components of the displacement vector field obtained using the mutual information similarity measure. One observes a good correlation between the horizontal component and the topography shown in fig. 2(c). As expected, the vertical (satellite along-track) direction does not show any particular structure. When this displacement vector field is used for the registration of the images, a good superposition is achieved. The detailed analysis of the procedure was carried out in (Inglada and Giros, 2004). If we analyze the distribution of the estimated shifts by computing their histograms, we observe the following behaviour (fig. 4): when the SPOT image is used as the reference, a high number of estimated shifts are multiples of 0.5 pixels; if the ERS image is used as the reference, this effect is attenuated and the shifts present a more uniform distribution. Since the similarity measure is the same for both cases and so is the optimization procedure, one can conclude that the subpixel shifts artifacts appear when the ERS image is interpolated during the similarity optimization. The following sections will study this effect in detail and a theoretical model for the origin of the artifacts will be presented.

4. ORIGIN OF THE ARTIFACTS

The problem of interpolation artifacts in the similarity surfaces has been studied for the case of mutual information-based medical image registration (Pluim, Maintz, and Viergever, 2000).

In this section we show that the origin of the observed artifacts is the interpolation procedure used for the subpixel registration. In this procedure, we resample the local image patches in order to measure the similarities for different shifted positions. The re-sampling is performed by image interpolation. In order to obtain a shift of $\delta < 1$ pixels, we have to estimate the image grey levels

at positions which lay between the samples of the image. The image to be resampled $x[n]$ is considered to be the sampled version of an ideal continuous image $x(t)$:

$$x[n] = x(nT),$$

where T is the sampling step. The shifted image $y[n]$ will be obtained by sampling the same original image $x(t)$ with a shifted sampling grid. Assuming that $x(t)$ was correctly sampled (with respect to the Shannon criterion) we can retrieve $x(t)$ from $x[n]$ by ideal interpolation, that is, by using a Sinc interpolator.

The Sinc interpolator has an infinite impulse response. Therefore approximate interpolators will be used. In order to increase computation speed, we want to use interpolation filters with a low number of samples.

For a linear interpolator, the interpolated image $y(t)$ for a shift δ will take the following expression:

$$y(t) = (1 - \delta)x(t - \delta) + \delta x(t + 1 - \delta), \quad (1)$$

and its Fourier transform is:

$$Y(f) = X(f) \left[(1 - \delta)e^{-j2\pi\delta f} + \delta e^{-j2\pi(\delta-1)f} \right]. \quad (2)$$

We see that the interpolated signal $y(t)$ is not exactly equal to the original signal $x(t)$ due to the fact that we are not using an ideal interpolator. Instead, we obtain a low-pass filtered version of the original signal. It is interesting to note that the blurring of the image introduced by the interpolation depends on the shift. Fig. 5(a) shows that the blurring effect increases when the shift comes close to half a pixel ($\delta = 1/2$).

This means that in the case of noisy images, the interpolation has a denoising effect and therefore, it increases the quality of the similarity estimation. Since this blurring is not the same for every shift, the similarity surface may show low values for a null shift (no blurring) and higher values for shifts close to half a pixel (strong blurring). It is important to note that the artifacts do not come from the blurring effect itself, but rather from the difference of blurring effect for different shift values.

Its is now interesting to analyze this effect for other interpolators. For the case of an interpolator $c(t)$ truncated to 4 samples, the Fourier transform of the interpolated signal takes the following expression:

$$Y(f) = X(f) \left[c(\delta + 1)e^{-j2\pi(\delta+1)f} + c(\delta)e^{-j2\pi\delta f} + c(1 - \delta)e^{-j2\pi(1-\delta)f} + c(2 - \delta)e^{-j2\pi(2-\delta)f} \right] \quad (3)$$

For the case of a Sinc interpolator, $c(t) = \frac{\sin(\pi t)}{\pi t}$. The frequency response of the interpolator as a function of the shift δ is shown in fig. 5(b). We see that the blurring effect is still dependent on the shift, but also that for such a short filter the continuous frequency is also filtered. This can produce effects which are worse than the linear interpolator. We will see this in the following sections.

Finally we analyze the case of a cubic B-Spline interpolator. In this case, the filter coefficients take the following expression:

$$c(t) = \begin{cases} \frac{2}{3} - \frac{1}{2}|x|^2(2 - |x|) & 0 \leq |x| < 1; \\ \frac{1}{6}(2 - |x|)^3 & 1 \leq |x| < 2; \\ 0 & |x| > 2; \end{cases} \quad (4)$$

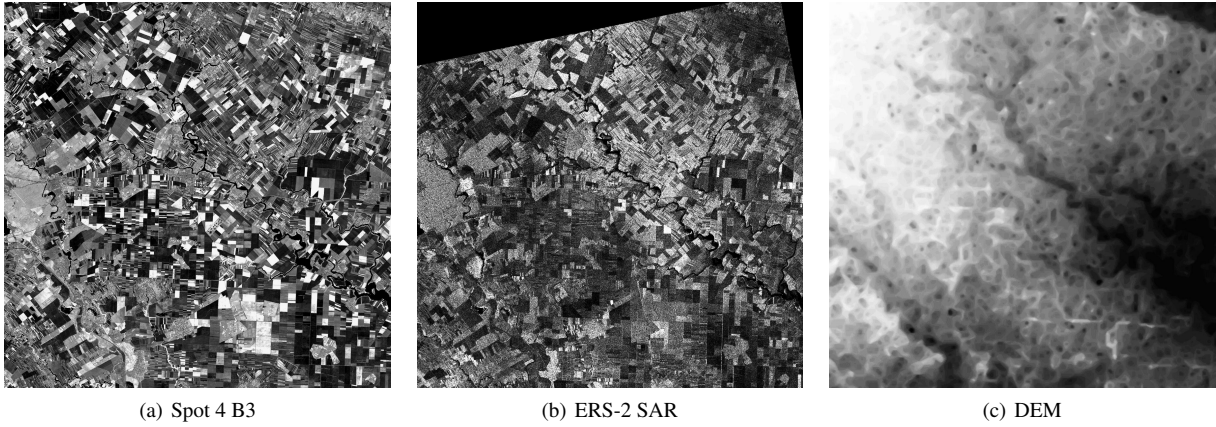


Figure 2. Images and DEM for the test area.

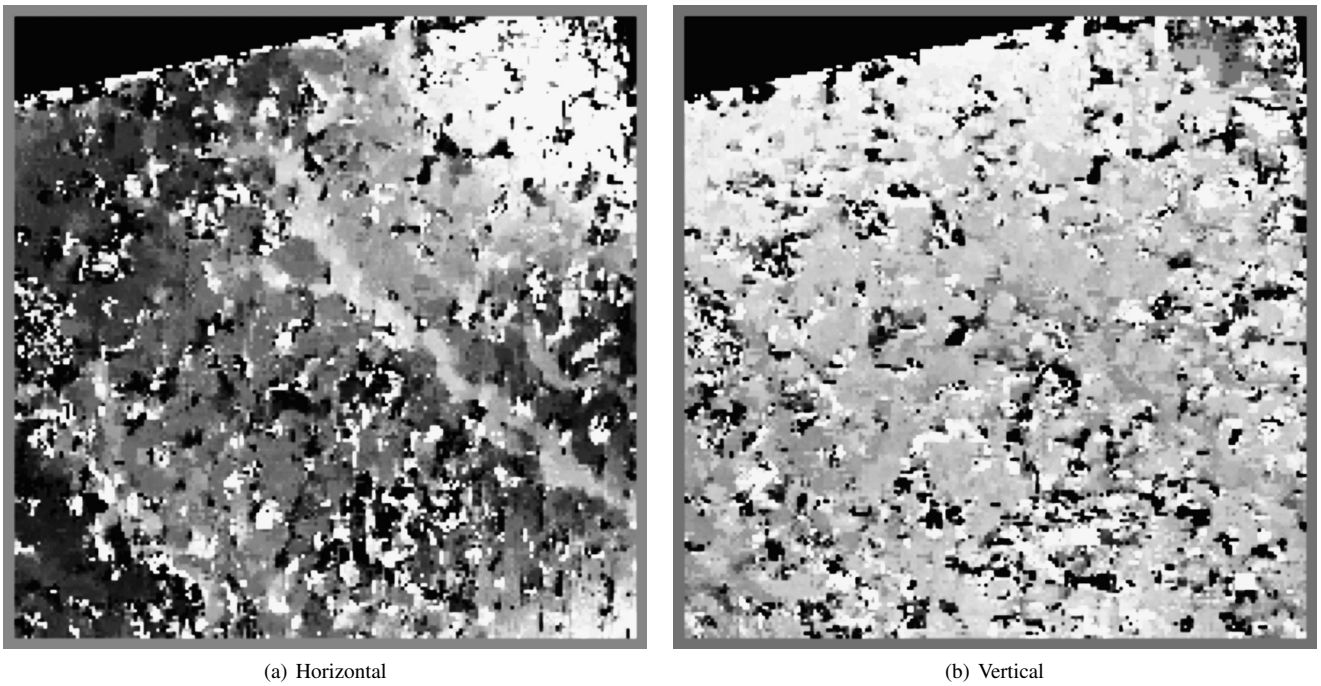


Figure 3. Deformation grid. Mutual information, estimation window is 51×51 pixels, sampling rate is 5 pixels.

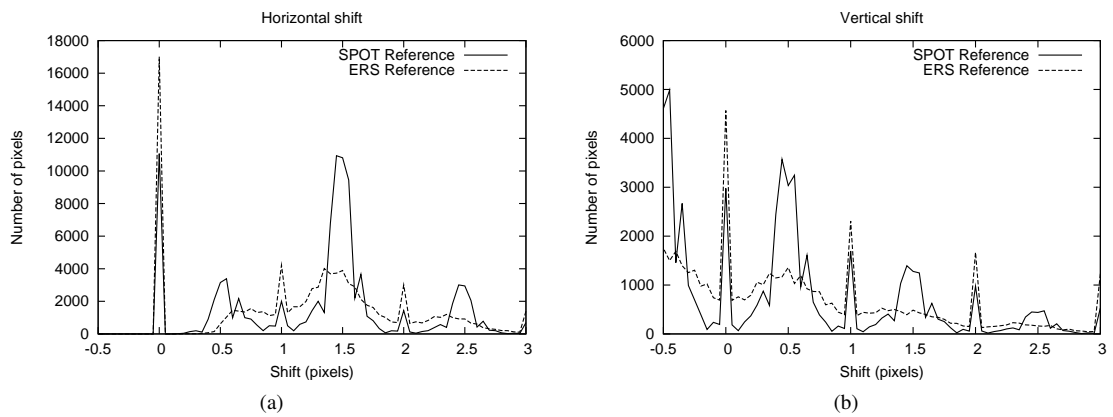


Figure 4. Histograms of the estimated subpixel shifts [(a) horizontal and (b) vertical] with inversion of the reference and the secondary images

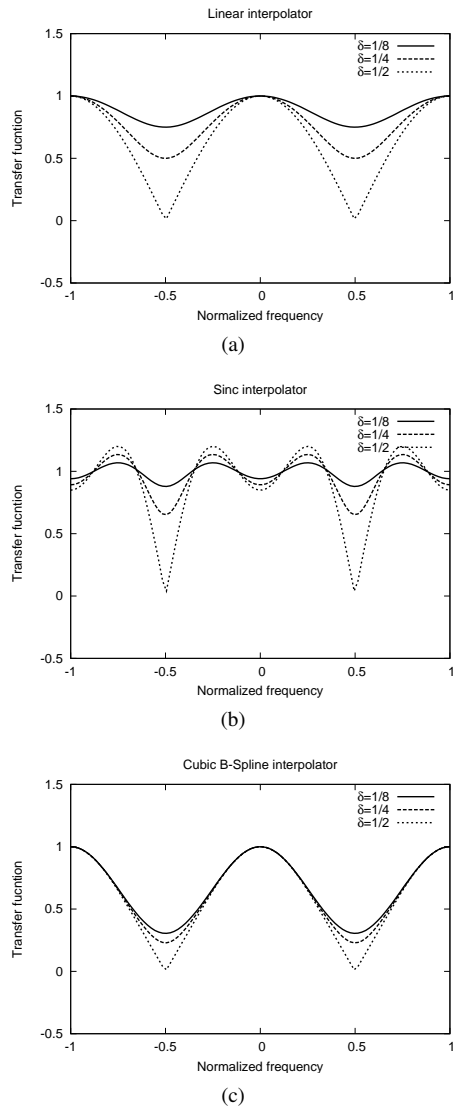


Figure 5. Evolution of the blurring effect of the interpolators as a function of the shift: (a) linear; (b) truncated Sinc; (c) cubic B-Spline.

Fig. 5(c) shows the frequency response of the 4-sample cubic B-Spline interpolator. We can see that the blurring effect remains nearly the same for all shifts.

4.1 Sensitivity analysis

We analyze here the behaviour of the different interpolators and their effects on the similarity functions. The similarity function is defined as the value of the similarity measure as a function of the shift. Without loss of generality, we will apply the shifts in only one direction. In this case, the similarity function can be plotted as a one-dimensional function. This analysis will be done for the two similarity measures, the correlation coefficient and the mutual information. The data used for these experiments is a SPOT 4 image which is compared to a noisy version of itself. This allows us to ensure that the images are perfectly co-registered. Additive white Gaussian noise has been added to the secondary image with a SNR of 100dB. Fig. 6 shows the similarity functions for four different interpolators, the three studied in the previous section, plus a sinus cardinal of length equal to 10 samples, which is a better approximation of the ideal one. For the case of the correlation coefficient (fig. 6(a)) we obtain a behaviour which could

be predicted from the theory presented above. The linear and the Sinc-4 interpolators have strong maxima close to the half-pixel shifts. We can observe that these effects are much weaker for the B-Spline interpolator and that they are nearly inexistent for the Sinc-10 one. It is worth to notice that the erroneous maxima are not exactly located on the half-pixel shifts and that they are not symmetrical with respect to the null translation. This is caused by the fact that we are measuring the similarity between an image and its noisy-shifted-blurred version with a degree of blurring which depends on the shift. The blurring is useful for denoising, thus for increasing the similarity. On the other hand, the shift decreases the similarity, because the homologous pixels are further away. Therefore, the combination of these two effects may produce a similarity maximum whose location depends on the local content of the image.

This is the case for the mutual information plots shown on fig. 6(b). As discussed in (Inglada and Giros, 2004), mutual information peaks have a higher slope that correlation coefficient ones. That means that the effect of erroneous peaks will only appear for interpolators whose behaviour is very sensitive to the shifts. Also, one could expect that the erroneous maxima will appear near to the null shift. This is what can be observed in the plots. For the linear interpolator, the peaks appear for about one third of a pixel. We can also observe that, since mutual information is able to measure the dependence in the presence of noise, the global maximum is located at 0, even if its value is not much higher than the secondary maxima. For the case of interpolators with a more stable smoothing, one can see that there is no clear peak, meaning that the smoothing effect produces a high value of mutual information even for shifts larger than half a pixel. Of course the mutual information value is low for integer pixel shifts, since no interpolation is applied in this case.

We can also analyze the influence of the noise level on the similarity functions. Since the registration functions of figure 6 show only the behaviour for a selected pixel of the image, it is difficult to infer the global quality of the registration from them. In order to study the global quality, we will analyze the histograms of the estimated shifts. We will study the different combinations of interpolators (linear, cubic B-Spline and Sinc-10), similarity measures (correlation coefficient, mutual information) and noise level. The results (for correlation only) are shown in figure 7. As for the previous simulations, only one one-dimensional shifts have been applied. In terms of noise influence, one observes that, the higher the SNR, the lower the number of shifts multiple of 0.5 pixels. We also observe that, when the SNR increases, the peaks move close to the null shift. If we compare the interpolators for a given SNR, say 15 dB, we see that, the better the interpolator (linear is worst, then B-Spline, and Sinc-10 is best), the higher the number of pixels for which the estimated shift is close to 0, the expected value. This is true for both similarity measures.

5. ATTENUATION OF THE ARTIFACTS

As it has been stated above, we are interested in using short interpolating filters, since the interpolation is performed a high number of times during the similarity optimization procedure. As we have shown above, the interpolation artifacts are produced by the blurring effects of the interpolators. More precisely, the origin of the artifacts is not the blurring effect itself, but rather the difference of blurring intensity as a function of the applied shift. We have shown, for instance, that, even if the B-Spline interpolator

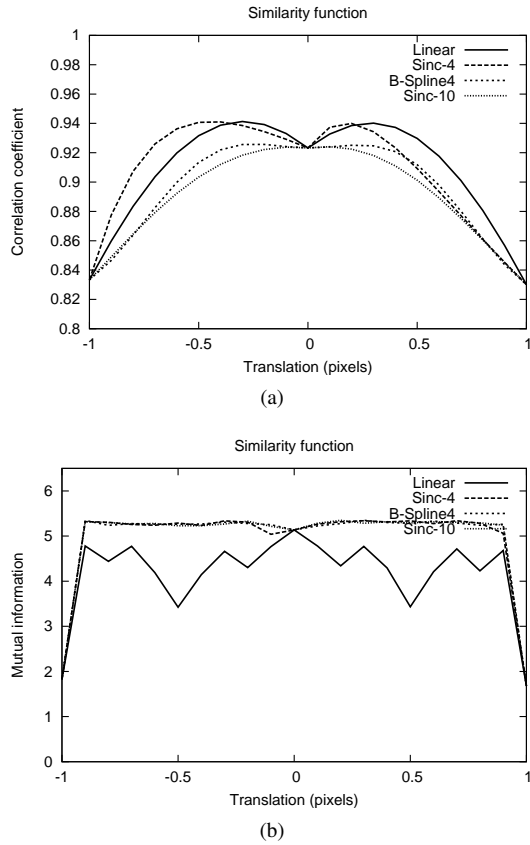


Figure 6. Comparison of interpolators

has a stronger blurring effect than the linear interpolator, since its blurring remains nearly constant for all shifts, it has better performances for the disparity map estimation. The strategy proposed here for reducing the interpolation artifacts is a very simple one. Since, the interpolator is going to introduce a blurring effect, we can smooth the secondary image with a filter whose transfer function is identical (in modulus) to the maximum blurring effect of the interpolator. This can be done in a pre-processing step. However, when observing fig. 5, we see that the evolution of the blurring effect may not be only related to the highest frequencies of the signal, and, therefore, selecting the transfer function of the pre-processing filter could be tricky. For instance, choosing a simple boxcar filter for pre-processing, can produce artifacts introduced by the secondary lobes of the filter. These lobes come from the windowing used for the truncation of the filter's impulse response.

In order to study the improvement of the subpixel shift estimation for the different interpolators, we choose to use the same smoothing filter for all of them. In order to reduce the secondary lobes of the smoothing filter and assuring a short impulse response, we propose to use a prolate function (Slepian, 1978). The prolate filter is one of the class of non recursive finite impulse response filters. It is superior to other filters in this class in that it has maximum energy concentration in the frequency passband and minimum ringing in the time domain. A prolate filter with 7 samples is shown in figure 8 and compared to the maximum smoothing for several interpolators. The frequency response of the 7×7 boxcar filter, with its secondary lobes is also shown. Fig. 9 shows the same kind of analysis as fig. 7, but with the use of the prolate filter as a pre-processing step for the secondary image. The first remark we can make is that the peaks at multiples of 0.5 pixels have vanished for both similarity measures and for all interpola-

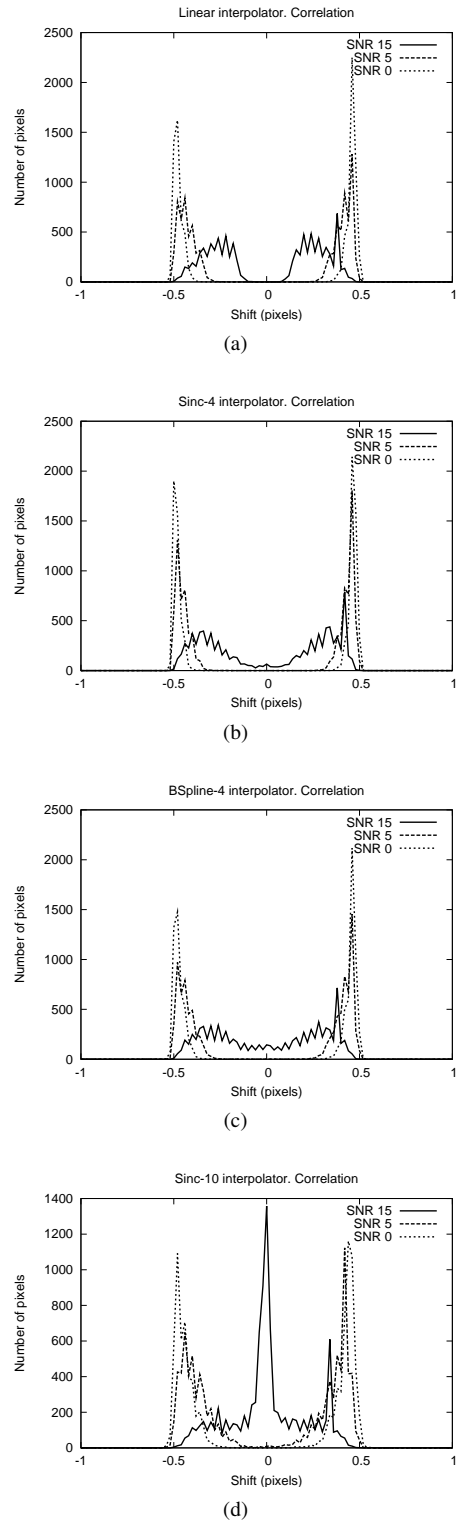
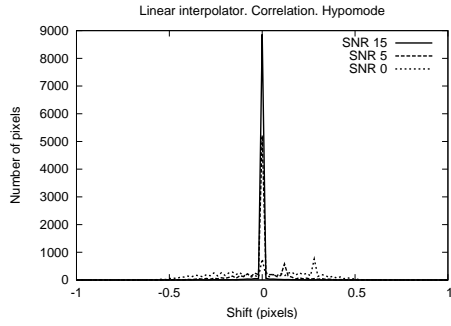
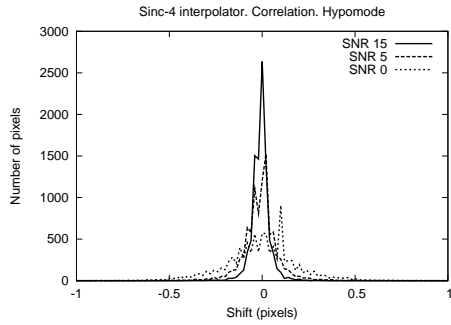


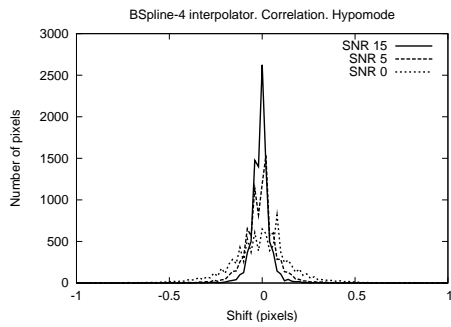
Figure 7. Influence of noise level on the estimated shifts.



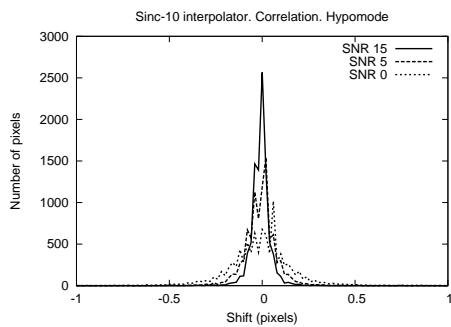
(a)



(b)



(c)



(d)

Figure 9. Influence low-pass filtering on the estimated pixel shifts for different noise levels

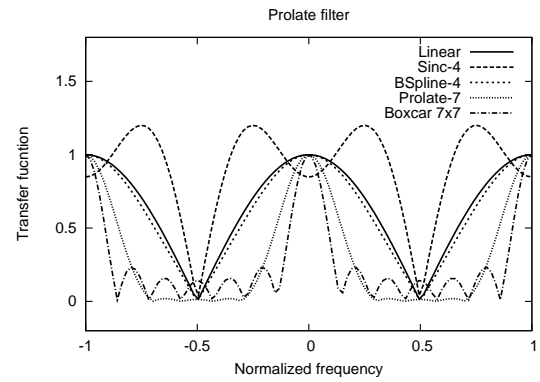


Figure 8. Frequency response of the smoothing prolate filter compared to different interpolators for $\delta = 1/2$. The 7×7 boxcar filter is also shown

tors. We also see that for the high SNR values, the best results are obtained for the linear interpolator. However, for low SNR values, the better the interpolator, the better the estimated shifts.

6. CONCLUSION

This paper has presented the problem of interpolation-induced artifacts in the procedure of disparity map estimation used for subpixel image registration. The problem has been introduced with a real case, where the presence of wrongly estimated shifts when a radar image is interpolated have been shown. A theoretical explanation of the origin of the artifacts has been given and it demonstrated that the blurring effect of the interpolator, which is dependent on the applied shift, is the responsible for the errors observed in the registration functions. Several interpolators have been compared under different SNR conditions. Finally, it has been shown that a pre-processing step which smoothes the secondary – interpolated – image can solve the problem. However, attention has to be paid to the choice of the smoothing filter. Indeed, simple filters as the boxcar one, have to be avoided since they present secondary lobes for the frequencies where the interpolation artifacts occur.

ACKNOWLEDGEMENTS

This research was supported by the French Centre National d'Études Spatiales, CNES, under contract 4500013574/DCT094.

REFERENCES

- Inglada, J. and Giros, A., 2004. On the possibility of automatic multi-sensor image registration. *IEEE Transactions on Geoscience and Remote Sensing* 42(10), 2104–2120.
- Pluim, J. P. W., Maintz, J. B. A., and Viergever, M. A., 2000. Interpolation Artefacts in Mutual Information-Based Image Registration. *Computer Vision and Image Understanding* (77), 211–232.
- Slepian, D., 1978. Prolate spheroidal wave functions, Fourier analysis, and uncertainty- V: The discrete case. *Bell System Tech. J.* 57, 1371–1429.